Average scattering matrix elements from high resolution neutron total cross sections for ^{32}S

C. H. Johnson

Oak Ridge National Laboratory, Oak Ridge, Tennessee 37830

R. R. Winters

Denison University, Granville, Ohio 43023

(Received 11 August 1982)

A previous analysis of high resolution measurements of the total cross sections for 25- to 1100-keV neutrons on ^{32}S in terms of an *l*-dependent optical model is extended to obtain model-independent but still *l*-dependent average scattering matrix elements from the data. The particular optical model obtained here is essentially the same as that deduced in the previous paper but the matrix elements are more amenable to future analyses with different models.

[NUCLEAR REACTIONS ^{32}S(n,n), $E_n = 25-1100$ keV, average scattering matrix elements and optical model parameters for $l = 0$ and 1.]

In the last quarter century since Barschall's pioneering comment[1] on averaged experimental neutron cross sections and Feshbach, Porter, and Weisskopf's interpretation[2] in terms of an optical model potential, there have been many papers with varying degrees of sophistication in which averaged cross sections are described by various optical models. Two years ago we reported[3] a set of parameters for a spherical but *l*-dependent potential that adequately described two average experimental quantities for each *l* and *J*, the strength function s_{lJ}, and the external R function R_{lJ}^{ext}, which had been deduced by partial wave analysis of high resolution measurements of total cross sections for ^{32}S $+ n$. Those two quantities were chosen in part because they are familiar to workers in neutron physics. However, since s_{lJ} and R_{lJ}^{ext} involve the rather arbitrary R-matrix boundary conditions used for analyzing the data, the optical model calculation of s_{lJ} and R_{lJ}^{ext} had to include those same boundary conditions. In fact, a comparison of any model to the experiment via those functions must take into account the choice of boundary conditions.

MacDonald[4] suggested that the high resolution neutron data be analyzed to produce an average scattering matrix element for each *lJ*. Since such averages are independent of boundary conditions, the adjustment of the model can proceed without reference to those conditions. Such is the purpose of this Brief Report. Of course, the two procedures are essentially equivalent and each has its merit. The comparison of the data to nuclear models via s_{lJ} and R_{lJ}^{ext} shows more clearly the relationship of the theory to the experiment, but the average matrix elements may be more amenable to future theoretical interpretation because they do not involve the arbitrary channel radius.

In Fig. 1 is shown schematically the chain of logic of our procedure. The upper and lower branches begin, respectively, with the data and model. Taking the upper branch first, consider the data block. High resolution total cross sections for neutrons on sulfur (95% ^{32}S) were measured[5] over an energy interval (designated *I*) from 25 to 1100 keV using the Oak Ridge neutron time-of-flight facility, ORELA. Ideally, angular distributions would be included, but the total cross sections are adequate here because ^{32}S has zero spin and only the entrance neutron channel is important.

The second block denotes the R-matrix multilevel fitting[3,5] of the data. Only the $s_{1/2}$, $p_{1/2}$, and $p_{3/2}$ channels were considered; the barriers for higher partial waves restrict their contribution to very narrow resonances. For channel *lJ* the scattering matrix element can be written in the R-matrix formalism[6,7] as

$$S_{lJ}(E) = e^{-2i\phi_l}(1 - L_l^* R_{lJ})/(1 - L_l R_{lJ}) , \qquad (1)$$
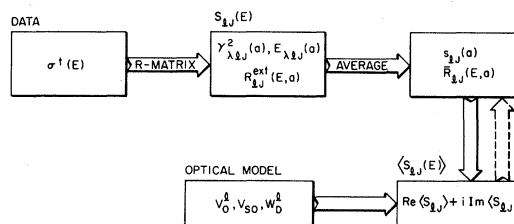

FIG. 1. Schematic diagram of the chain of logic from high resolution total cross sections to an optical model potential. In the previous report (Ref. 3) the model was compared to experiment in the upper right block; here the comparison is made in the lower right block so that the R-matrix boundary conditions are not involved in the model. The boundary conditions are indicated by the boundary radius a.

where all terms on the right are evaluated at the chosen boundary radius a. At energy E, ϕ_l is the hard sphere phase shift, $L_l = S_l - B_l + iP_l$, S_l is the shift factor, P_l is the penetrability, and B_l a chosen boundary condition. As previously, we choose $B_l = S_l$. The R function is then subdivided into a sum over the levels in the interval I plus a term for all external levels;

$$R_{lJ}(E) = \sum_I \gamma_{\lambda lJ}^2/(E_{\lambda lJ} - E) + R_{lJ}^{\text{ext}}(E) , \quad (2)$$

where $\gamma_{\lambda lJ}^2$ and $E_{\lambda lJ}$ are the reduced width the eigenenergy for the level λ.

The R_{lJ}^{ext} must increase monotonically and smoothly in the region. In principle, this function can be obtained exactly from the fitting procedure; however, the quality of the data is such that it is very well determined for $s_{1/2}$ and less well for $p_{1/2}$ and $p_{3/2}$. As in our previous paper,[3] we expand R_{lJ}^{ext} in a form which is appropriate[6-8] for the subsequent averaging:

$$R_{lJ}^{\text{ext}}(E) = \overline{R}_{lJ}(E) - \text{Pr} \int_I s_{lJ} dE'/(E' - E) , \quad (3)$$

where the strength function s_{lJ} is set equal to that observed in the interval, and the real smoothed R function[6] is parametrized as a first order polynomial:

$$s_{lJ} = \langle \gamma^2/D \rangle_{lJ} , \quad (4)$$

$$\overline{R}_{lJ}(E) = \alpha_{lJ} + \beta_{lJ}E , \quad (5)$$

and D is the average level spacing. The fitted values of α_{lJ}, β_{lJ}, and $\langle \gamma^2/D \rangle_{lJ}$ are listed in Table II of Johnson and Winters.[3] In Eq. (3), Pr denotes the principal part of the integral. The subtraction of this integral is equivalent to the addition of the integral from $-\infty$ to $+\infty$, with the interval I excluded. Froehner[9] has also emphasized the importance of Eq. (3).

For the moment we leave the upper branch in Fig. 1 and consider the block labeled "optical model." Modern models have many parameters but the present data justify only two adjustable parameters for each partial wave. As discussed previously,[3] we fix the geometries for a Woods-Saxon well with surface-derivative imaginary and spin-orbit terms and then adjust only the well depths for each partial wave. For given well depths we calculate the optical model scattering matrix elements as indicated in the lower right block in Fig. 1.

In our previous paper, as indicated by the dashed arrow in Fig. 1, we expanded the scattering matrix in terms of a smoothly varying complex R function[6,7] using the same boundary conditions as above:

$$S_{lJ}^{\text{OMP}} = e^{-2i\phi_l}(1 - L_l^* \mathfrak{R}_{lJ})/(1 - L_l \mathfrak{R}_{lJ}) , \quad (6)$$

where

$$\mathfrak{R}_{lJ}(E) = \overline{R}_{lJ}(E) + i\pi s_{lJ}(E) . \quad (7)$$

We then adjusted the model well depths to give a good fit of the predicted s_{lJ} and $\overline{R}_{lJ}$ from Eq. (7) to those observed in Eqs. (4) and (5).

In the present paper we simply reverse part of the procedure, as indicated by the solid downward arrow in Fig. 1. Thus we insert the experimental $\overline{R}_{lJ}(E)$ and s_{lJ} in the right hand side of Eq. (6) in order to find the experimental average $\langle S_{lJ} \rangle$, which are to be fitted by the optical model predictions. The results could be displayed in various ways. Our choice is to plot quantities proportional to the average shape elastic and compound cross sections:

$$\sigma_{lJ}^{se}/g_J = \pi k^{-2}|1 - \langle S_{lJ} \rangle|^2 , \quad (8)$$

and

$$\sigma_{lJ}^{c}/g_J = \pi k^{-2}(1 - |\langle S_{lJ} \rangle|^2) , \quad (9)$$

where g_J is the statistical factor $J + \frac{1}{2}$, for a spin-zero nucleus. In Figs. 2 and 3 the solid curves show these average quantities deduced from the data.

The dashed curves in Figs. 2 and 3 are the best visual fits of the model to the data. The resulting well depths are listed in the figures. The uncertainties are approximately ± 1 MeV for V_0 and ± 1.5 MeV for W_D.[3] The model geometries were fixed as the previous work[3] with 1.21 fm for all radii and with $a_0 = 0.66$ fm and $a_D = 0.48$ fm. As expected, the well
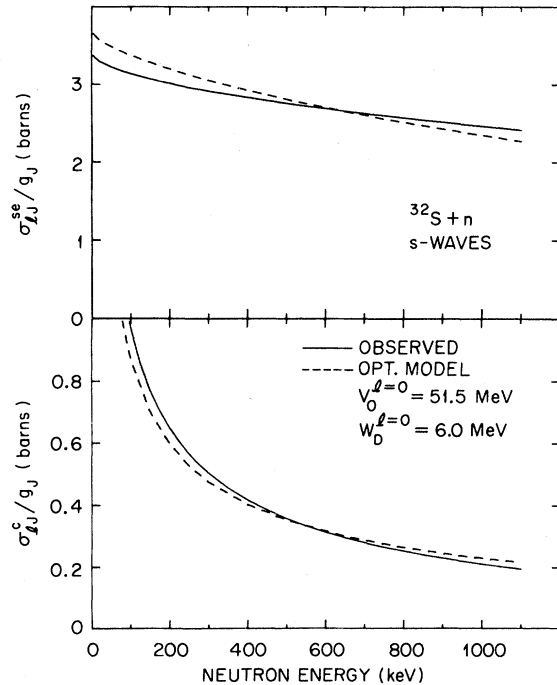

FIG. 2. Average experimental s-wave shape elastic and compound cross sections (divided by g_J) and visually adjusted predictions from an optical model. The potential geometries are as in Ref. 3 with all radii at 1.21 fm and with $a_0 = 0.66$ fm and $a_D = 0.48$ fm.
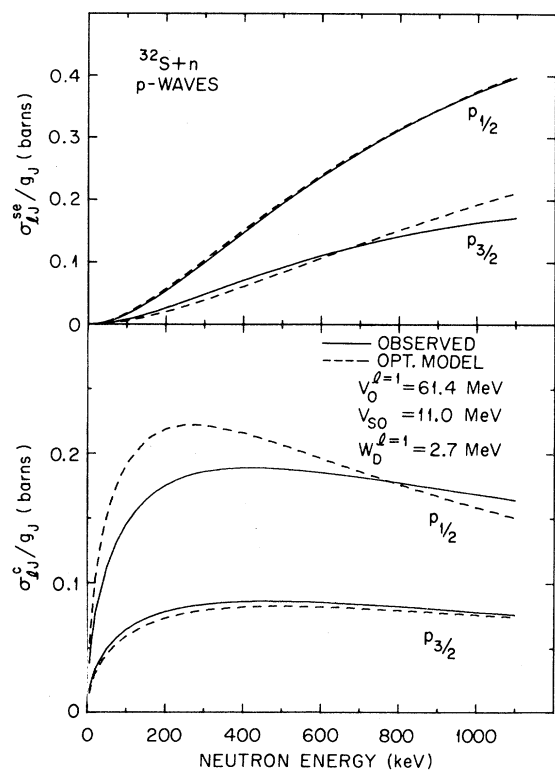
FIG. 3. Same as Fig. 2 but for p waves.

parity or l dependence. Of particular interest is that for the real part; the V_0 is 10 MeV greater for p waves than for s waves. This result, which comes primarily from fitting the real parts of the scattering matrix elements, means that the spherical well demands different depths for s and p waves to properly locate the $2p$ and $3s$ single particle states. As we have already discussed,[3] the parity dependence is also required to give the observed binding energy for the $2p$ states and the mass location of the $3s$ size resonance.

For the imaginary part of the potential, a parity dependence is suggested by the s- to p-wave ratio of $2/1$ for W_D. However, we emphasize that each W_D has a large uncertainty because it has been deduced primarily from $\langle \gamma^2/D \rangle$, a quantity which has a large inherent uncertainty resulting from Porter-Thomas fluctuations. If N levels are drawn from a Porter-Thomas distribution, the fractional uncertainty in $\langle \gamma^2/D \rangle$ is $(2/N)^{1/2}$; in the present case N is only 5, 7, and 8 for $s_{1/2}$, $p_{1/2}$, and $p_{3/2}$, respectively. We also note that such few levels provide little evidence for the energy dependence of the strength function. Thus each experimental s_{lJ} has been assumed constant, whereas the model s_{lJ} is energy dependent. For this reason no significance is given to the difference in shapes of the model and experimental curves for σ^c in Figs. 2 and 3. The difference is particularly large for the $p_{1/2}$ curves because the model strength is on the high energy side of the nearby $2p_{1/2}$ bound state.

depths are nearly the same as deduced previously. The main differences result because the present and previous potentials actually had slightly different geometries; the same Wood-Saxon geometry parameters were used in both cases but previously the potentials were set to zero outside the 6.4-fm R-matrix boundary. In fact, one purpose of this Report is to give well depths for a model without a cutoff.

The most striking feature of our model is a strong

[1]H. H. Barschall, Phys. Rev. <u>86</u>, 431 (1952).

[2]H. Feshbach, C. E. Porter, and V. F. Weisskopf, Phys. Rev. <u>96</u>, 448 (1954).

[3]C. H. Johnson and R. R. Winters, Phys. Rev. C <u>21</u>, 2190 (1980).

[4]W. M. MacDonald, C. H. Johnson, and R. R. Winters, Bull. Am. Phys. Soc. <u>26</u>, 1139 (1981).

[5]J. Halperin, C. H. Johnson, R. R. Winters, and R. L. Macklin, Phys. Rev. C <u>21</u>, 545 (1980).

[6]A. M. Lane and R. G. Thomas, Rev. Mod. Phys. <u>30</u>,

257 (1958).

[7]J. E. Lynn, *The Theory of Neutron Resonance Reactions* (Clarendon, Oxford, 1968).

[8]C. H. Johnson, N. M. Larson, C. Mahaux, and R. R. Winters, Phys. Rev. C (to be published).

[9]F. H. Froehner, in *Proceedings of the Conference on Nuclear Data Evaluation Methods and Procedures*, BNL Report No. BNL-NCS-51363, *I*, 375, edited by B. A. Magurno and S. Pearlstein (Brookhaven National Laboratory, September, 1980).